Hindawi
Geofluids
Volume 2022, Article ID 4168918, 24 pages
https://doi.org/10.1155/2022/4168918

Research Article

Experimental Study on Compressive and Flexural Performances of Polypropylene Fiber-Reinforced Concrete

Yimeng Wei,[1] Yuan Qin,[1] Junrui Chai,[1] Chengyong Xu,[2] Yue Zhang,[3] and Xianwei Zhang[4]

[1]*Institute of Water Resources and Hydro-Electric Engineering, Xi'an University of Technology, China*
[2]*Lianyungang Industrial Investment Group Xuwei Investment Co., Ltd., China*
[3]*Xianyang Research Institute of Water Conservancy and Hydropower Planning and Design, China*
[4]*Intelligent Environmental Protection Integrated Command Center, Xi'an Bureau of Ecology and Environment, China*

Correspondence should be addressed to Yuan Qin; qinyuan@xaut.edu.cn

Received 3 January 2022; Revised 24 March 2022; Accepted 8 September 2022; Published 23 September 2022

Academic Editor: Basim Abu-Jdayil

Plain concrete (PC) has the disadvantages of easy cracking and low resistance to deformation. In practical engineering, steel fiber or polymer fiber is usually selected to improve the tensile and crack resistance of concrete. In this study, the polypropylene fiber (PPF) was added to the concrete with the content of 0, 0.6, 0.9, and 1.5 kg/m^3. The compressive and flexural tests of PC and PPF-reinforced concrete (PPFRC) at 14, 28, and 60 days of curing were conducted. As the result, when the content of PPF exceeds to 1.2 kg/m^3, the workability became worse. The compressive and flexural strength of PPFRC increased compared with PC. However, the increase of strength does not always increase with the increase of fiber content. The uniaxial compressive strength of the PPFRC with the PPF of 1.2 kg/m^3 is the optimal at 14- and 28-day ages, which is 20.56% and 11.24% higher than PC, respectively. PPFRC with the PPF of 0.9 kg/m^3 is best of all at 60 days, which is 19.68% higher than PC. The flexural strength of the PPFRC-0.9 is the highest. Furthermore, the CFEC and CTI of PPFRC are both higher than those of PC, indicating that it has significant crack resistance and toughness.

1. Introduction

Concrete is the most widely used building materials because of its many advantages. However, concrete is a brittle material and easily cracks [1–3]. Nowadays, polymers and fibers have been widely used to alleviate crack growth and development. The application of fiber in civil engineering not only improves the mechanical properties of components but also provides a new idea for solving the solid waste of waste fiber [4, 5]. The polypropylene fiber (PPF) is considered to be an effective method for improving the shrinkage cracking characteristics and toughness [6]. The randomly distributed fibers can act as internal reinforcement to enhance the properties of the concrete. The internal structure of the fiber-reinforced concrete is shown in Figure 1. These fibers can improve the toughness and tensile strength of concrete and inhibit the progress of cracking [7–12]. The initial cracks are usually the origin of concrete damage or performance deterioration. And PPF can effectively restrain the occurrence and development of initial cracks [13–17].

Fiber-reinforced concrete has certain superiority in practical engineering application because of its high strength and toughness [3, 18–20]. PPF has been widely used in engineering projects and has achieved good engineering benefits, for example, the 124.4 m high reinforced concrete-face-rockfill dam in Baixi Reservoir in Ningbo, China. The second stage face of Baixi Reservoir Dam is located in the area of water-level fluctuation. In winter, this dam is often affected by environmental factors, such as cold currents and strong winds, and the working conditions are relatively bad. In order to prevent cracks in the concrete surface and improve the capacity for resisting deformation, PPFRC was used in

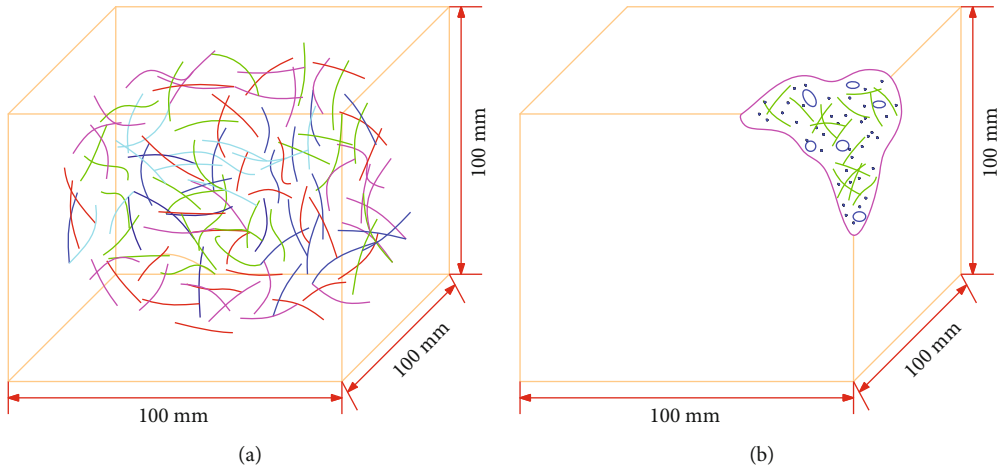

Figure 1: Internal structure of fiber-reinforced concrete.

Figure 2: PPF in the experiment.

Table 1: Physical properties of PPF.

Fiber type	PPF
Length (mm)	19
Diameter (μm)	31.2
Density (kg/m^3)	910
Tensile strength (MPa)	565
Elongation when break (%)	27
Elastic modulus (MPa)	5900
Melting point ($^\circ$C)	165
Water absorption	Null
Thermal conductivity	Very low
Electrical conductivity	Very low
Corrosion resistance to acid and alkali	Very strong

the second stage of the panel project, with a consumption of 11,000 m^3, including 9.9 tons of PPF.

Compressive strength is the most basic parameter in designing concrete structures [21–23]. And it has shown good correlation with other mechanical and physical properties. Scholars found that PPF can improve the tensile strength, flexural strength, and flexural toughness of concrete [24–27]. Some scholars believe that PPFRC has no significant effect on compressive strength because the fiber content is very low [18, 28]. Many scholars even think that adding PPF can lead to a slight decrease in the compressive strength of concrete [13, 28, 29]. The reason is that PPF has a low elastic modulus, leading to a slight decrease in compressive strength of PPFRC. However, other scholars argued that PPF can enhance the compressive strength of concrete [25, 30]. Fibers could reduce crack formation and development and thus led to increasing compressive strength [31]. Another advantage of adding fibers to concrete is that it improves the concrete durability, such as freeze-thaw resistance, impermeability, and chloride penetration resistance [18, 28, 32–36]. PPF can also improve the impact resistance and fatigue resistance of concrete [37, 38]. Due to its small diameter of PPF, the cement mortar of concrete matrix is covered with intersecting fiber filaments. Moreover, the between fibers and cement mortar have a strong bond [38]. Thus, concrete will not be destroyed immediately after initial cracking and can continue to bear loads. PPF increases the bond characteristics of cement mortar and the roughness of concrete surface to be repaired, reducing the generation of microcrack in concrete hardening [38–44].

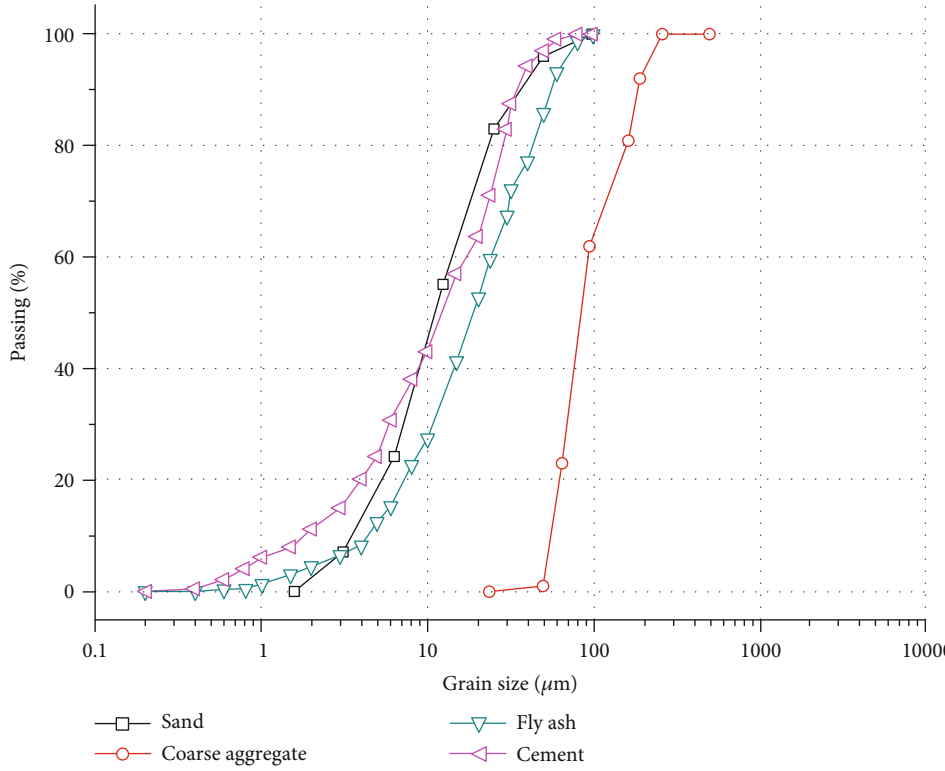

Figure 3: Gradation curves of cement, fly ash, and fine and coarse aggregates.

Table 2: Mix proportions of the PC and PPFRC mixtures.

Type	Cement (kg/m^3)	Sand (kg/m^3)	Fly ash (kg/m^3)	Coarse aggregate (kg/m^3)	Water (kg/m^3)	Water reducer agent (kg/m^3)	Fiber content (kg/m^3)
PC	275	815	90	1080	135	10	0
PPFRC-0.6	275	815	90	1080	135	10	0.6
PPFRC-0.9	275	815	90	1080	135	10	0.9
PPFRC-1.2	275	815	90	1080	145	12	1.2
PPFRC-1.5	275	815	90	1080	145	12.5	1.5

Table 3: Test type and specimen dimensions.

Test type	Dimensions (mm)	Number of specimens
Cube compression test	100 × 100 × 100	3 × 9 × 5
Uniaxial compression test	100 × 100 × 400	3 × 9 × 5
Flexural test	100 × 100 × 400	3 × 9 × 5

The performance of concrete at early age is very important for the control of project quality and progress. Previous studies mostly focused on the mechanics and durability of PPFRC after curing, but there were few studies on the development of mechanical properties of PPFRC during curing. In this study, the influence of PPF content on the working performance of concrete is considered. At the same time, the evolution and failure mechanism of mechanical properties of PPFRC with different content after standard curing for 14, 28, and 60 days are investigated. In addition, the constitutive model of PPFRC uniaxial compression tests with different ages optimized by difference algorithm was studied.

2. Experimental Program

2.1. Raw Materials. The materials for the preparation of PC and PPFRC specimens include cement, fly ash, tap water, graves, sand, water reducer, and PPF, wherein the size of gravels is 5–25 mm. PPF used in the experiment are

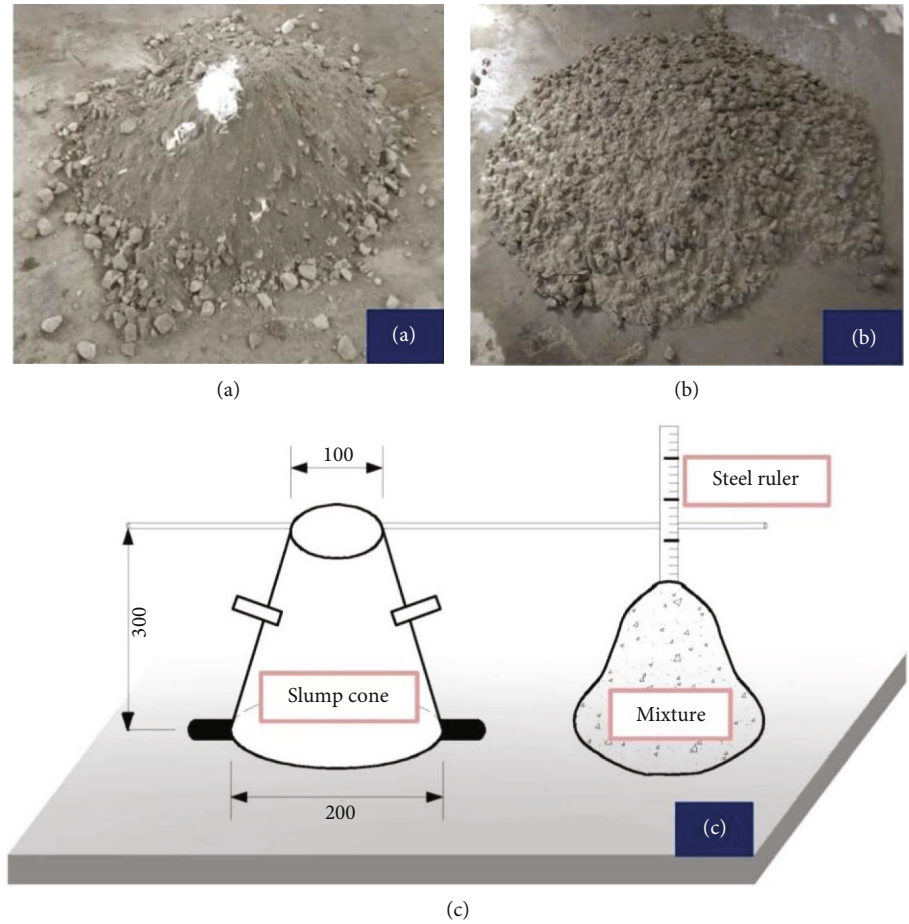

Figure 4: Concrete mixture and geometric diagram of slump cone.

Table 4: Properties of PC, PPFRC-0.6, PPFRC-0.9, PPFRC-1.2, and PPFRC-1.5.

Concrete type	Slumps (mm)	Water-binder ratio	Sand ratio	Density (kg/m^3)
PC	215	0.37	43%	2417
PPFRC-0.6	210	0.37	43%	2414
PPFRC-0.9	203	0.37	43%	2408
PPFRC-1.2	188	0.40	43%	2399
PPFRC-1.5	181	0.40	43%	2394

fascicular monofilaments, as shown in Figure 2. The PPF parameters used in the experiment are listed in Table 1.

2.2. Mix Design and Specimen Preparation. Concrete design strength used in the test is 30 MPa. A total of five concrete mixes were prepared. One PC mix and four PPFRC mixes containing PPF of 0.6, 0.9, 1.2, and 1.5 kg/m^3 were provided. The amounts of cement, sand, fly ash, and coarse aggregate were kept constant in all mixes. The gradation curve is shown in Figure 3. Notably, when the PPF content was 1.2 kg/m^3, the water consumption increased to 145 g. Furthermore, water reduction increased to 12 g. The mix designs of PPFRC and PC are shown in Table 2.

When preparing PC specimens, the coarse aggregate, sand, cement, and fly ash were first stirred for 2 min. After that, the water was poured into the mixture in three periods, and the mixture was stirred for 3 min. The gravels, sand, cement, fly ash, and PPF were stirred for 2 min, repeating the same process as PC specimens when preparing PPFRC specimens. Test the slump of PC and PPFRC mixture before pouring the mixture into the molds. Afterward, the mixture was injected into molds and vibrated evenly, and the molds were filled with unconsolidated PC and PPFRC were placed in moist air for 24 hours. The specimens are demoulded and numbered and cured for 14 days, 28 days, and 60 days in standard curing conditions. PPFRC with different fiber contents of 0.6, 0.9, 1.2, and 1.5 kg/m^3 were named PPFRC-0.6, PPFRC-0.9, PPFRC-1.2, and PPFRC-1.5, respectively. The test items and specimen dimensions used in this study are listed in Table 3.

2.3. Standard Slump Test and Density. The slump test was performed on fresh concrete mixture, and the weight of hardened concrete was measured at the same time. The geometry of a standard slump cone is shown in Figure 4, and the diameter of upper open mouth, the height, and the diameter of the bottom are 300, 100, and 200 mm, respectively. The difference of the maximum height of the fresh concrete mixture and the height of the slump cone was

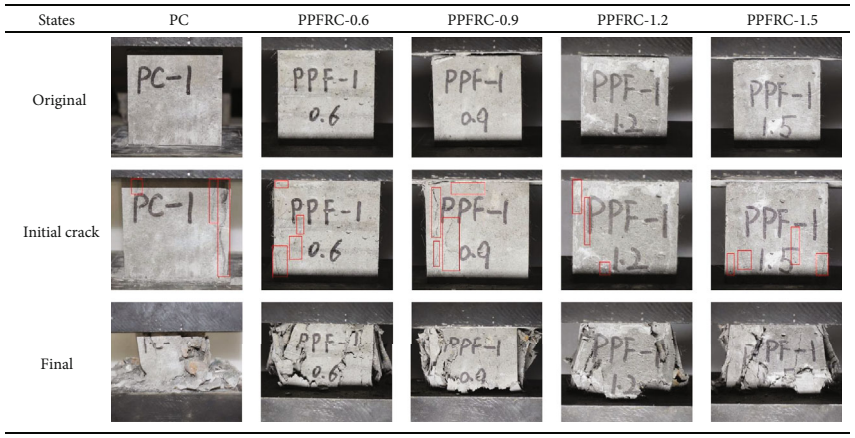

Figure 5: Macroscopic pictures of the initial crack, original, and final states of PC and PPFRC at 28 days of curing.

(a)

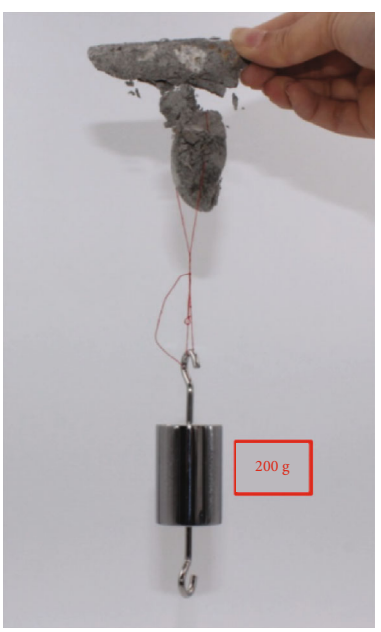

(b)

Figure 6: (a) The diagram for forming connecting bridge by fibers and (b) the weight of PPFRC fragment.

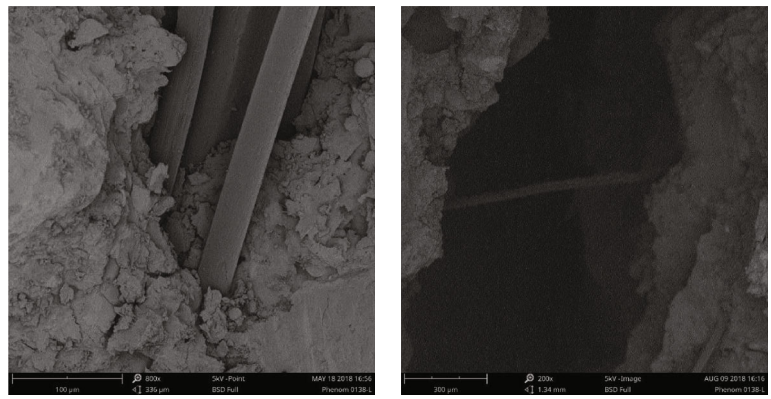

(a) (b)

Figure 7: The SEM images of (a) the fiber embedded in concrete mixture and (b) the fiber bridging crack.

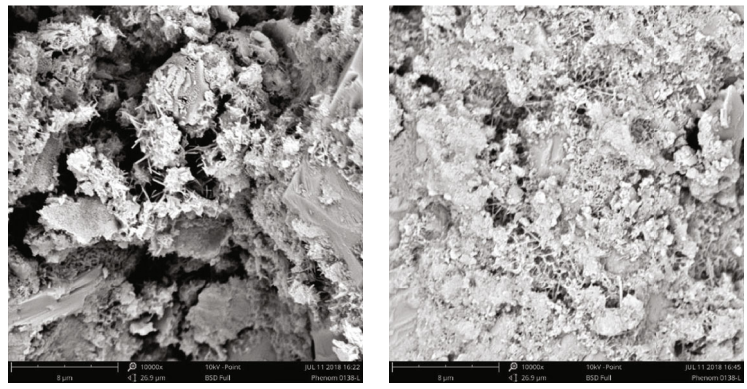

(a) PC (b) PPFRC

Figure 8: The SEM images of PC and PPFRC mixture at 60 days of curing (magnification 10000).

measured as the value of slump. The fluidity of the mixture is required in shotcrete engineering, and fiber has a significant effect on shotcrete performance. Moreover, the addition of fibers can effectively improve toughness and energy absorption capacity [45].

Taking PC as reference, the properties of PPFRC with different fiber contents are studied to examine the effect of fiber addition in the concrete. The effect of fibers on reducing the workability of the concrete mixes was measured by slump test. During mixing mixture, low-content PPF has a thickening effect on concrete mixture. The interfacial effect reduces the concrete segregation and improves the workability. However, if the PPF content exceeds 1.2 kg/m^3, the fluidity is poor, mixing is difficult, and the admixture and water consumption are both increased. With the increase of fiber content in concrete mixture, the processing performance of PPFRC mixes gradually declines [43]. The values of slump, water-binder ratio, sand ratio, and density for PC and PPFRC with different fiber contents are shown in Table 4. The average declines of PC, PPFRC-0.6, PPFRC-0.9, PPFRC-1.2, and PPFRC-1.5 are 215, 210, 203, 188, and 181 mm. The slumps of PPFRC-0.6, PPFRC-0.9, PPFRC-1.2, and PPFRC-1.5 are 2.33%, 5.58%, 12.56%, and 15.81% lower than that of PC. With the increase in fiber content, the slump was reduced due to interlock between gravels and fibers. This condition shows that PPF has a thickening effect on concrete mixes. The surface area of the fiber needs to consume a part of the cement slurry in the concrete, leading to a relative decrease in the amount of cement slurry in the surface area of the gravels and the decrease of the fluidity of the concrete mixture. The average weights of PC, PPFRC-0.6, PPFRC-0.9, PPFRC-1.2, and PPFRC-1.5 were 2,417, 2,417, 2,408, 2,441, and 2,394 kg, respectively. The reason for the different weight may be that the quantity or weights of the gravels are different or that the PPF takes up a certain amount of sand space, resulting in a decrease in sand content.

3. Test Results and Analysis

3.1. Cube Compression Test

3.1.1. Test Phenomena and Failure Patterns. The test was conducted according to the Chinese standard GB/T50081-2002. All the evaluation data were measured in 3 parallel samples under the same conditions, and the average value

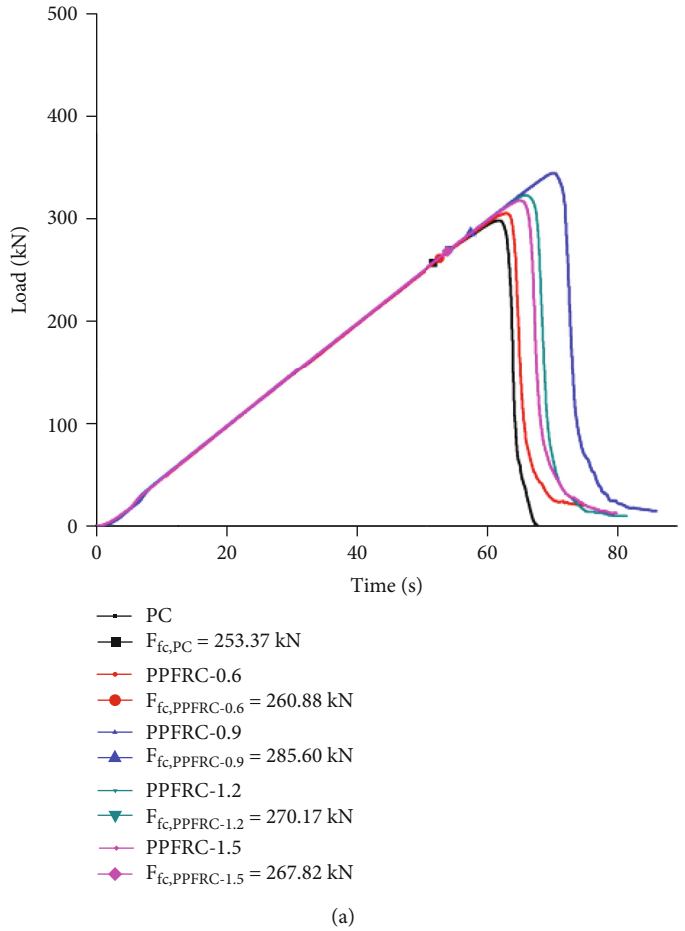

(a)

Figure 9: Continued.

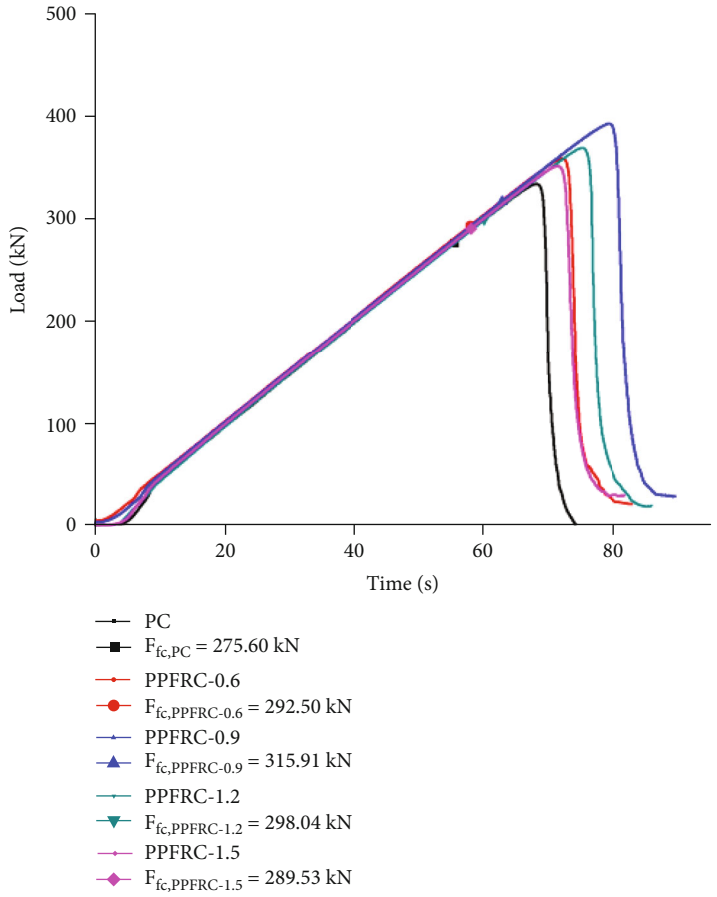

(b)

Figure 9: Continued.

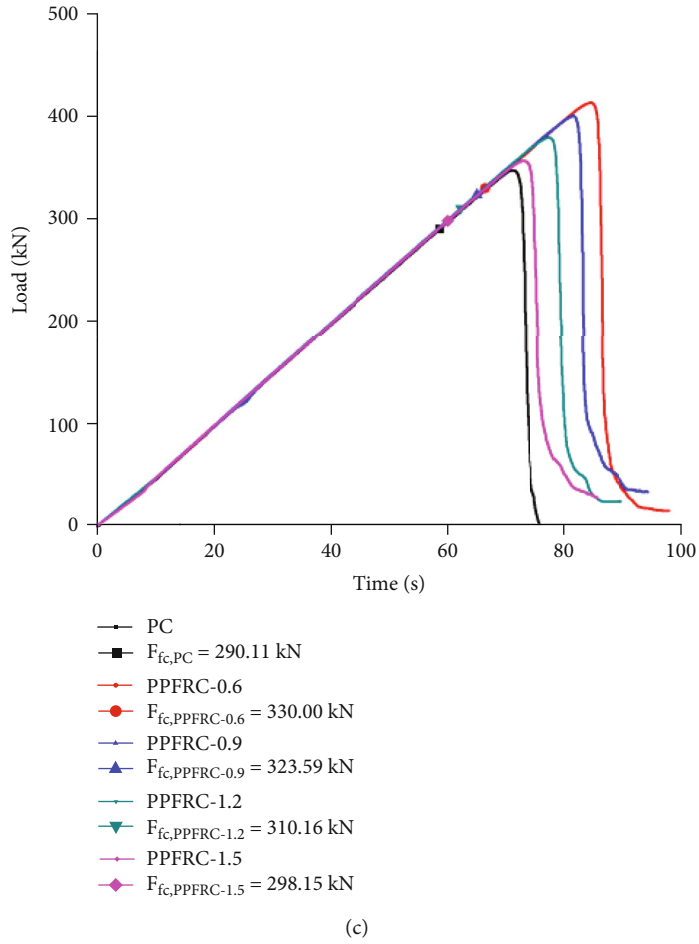

(c)

Figure 9: Load–time curves of PC and PPFRC from compressive test: (a) 14 days, (b) 28 days, and (c) 60 days.

was used in the discussion and analysis. Take the 28-day compressive test as an example. The macroscopic damage of PC, PPFRC-0.6, PPFRC-0.9, PPFRC-1.2, and PPFRC-1.5 after final unloading is exhibited in Figure 5. The fragments of the PC specimens are scattered, and the integrity is very poor. The structural support ability is also lost. On the contrary, some small fragments that are about to fall off are still bonded to the main body of the PPFRC specimens because of the bridging effect by fibers, and at this time, the specimens still have the ability to bear a less load. Large fiber content means the obvious integrity of the specimen after failure, indicating that PPF increases the deformation of specimen and the bearing capacity of specimen after cracking. During the test, addition of fibers increased the ductility of concrete damage, and the specimens remain intact from loading to failure. The fibers reduce the original cracks of concrete and inhibit the development of cracks of concrete. Therefore, the cracking load of fiber-reinforced concrete is larger than that of PC. Through qualitative analysis, when the concrete structure was damaged, PPFRC had the ability to delay the occurrence of the final damage due to the addition of fibers. This condition shows that PPF can greatly improve the crack resistance and toughness of concrete. The reason may be that PPF can prevent the development of the microcracks. During the test, when the specimens have been partially destroyed but not completely destroyed, the PPF exhibits a bridging effect and can still absorb a part of the energy.

PPF has a large specific surface area and has a strong bond with the cement base material. Figure 5(a) is a fragment of PPFRC, and PFF is uniformly dispersed and forms a chaotic system inside the concrete. As can been seen from Figure 6(a), it is clear that the fiber located in the width of formed crack like a connection bridges. The characteristic of fibers prevent the separation of concrete pieces after cracking. It can be seen that PPF plays the role of stirrups in PPFRC. Without considering the amount of fiber contained in the debris, it was found that after testing the 20 damaged fragments, the fiber can still exert a bridging effect after PPFRC is destroyed by pressure. As shown in Figure 6(b), through the rough measurement, the fibers can withstand the maximum weight of more than 200 g, which will be affected by the number of fibers contained between adjacent fragments, burying depth of fibers, and other related parameters, which is difficult to measure accurately.

3.1.2. SEM Results. The internal microscopic view of the specimens after destruction was scanned by scanning electron microscope (SEM). From a microscopic point of view,

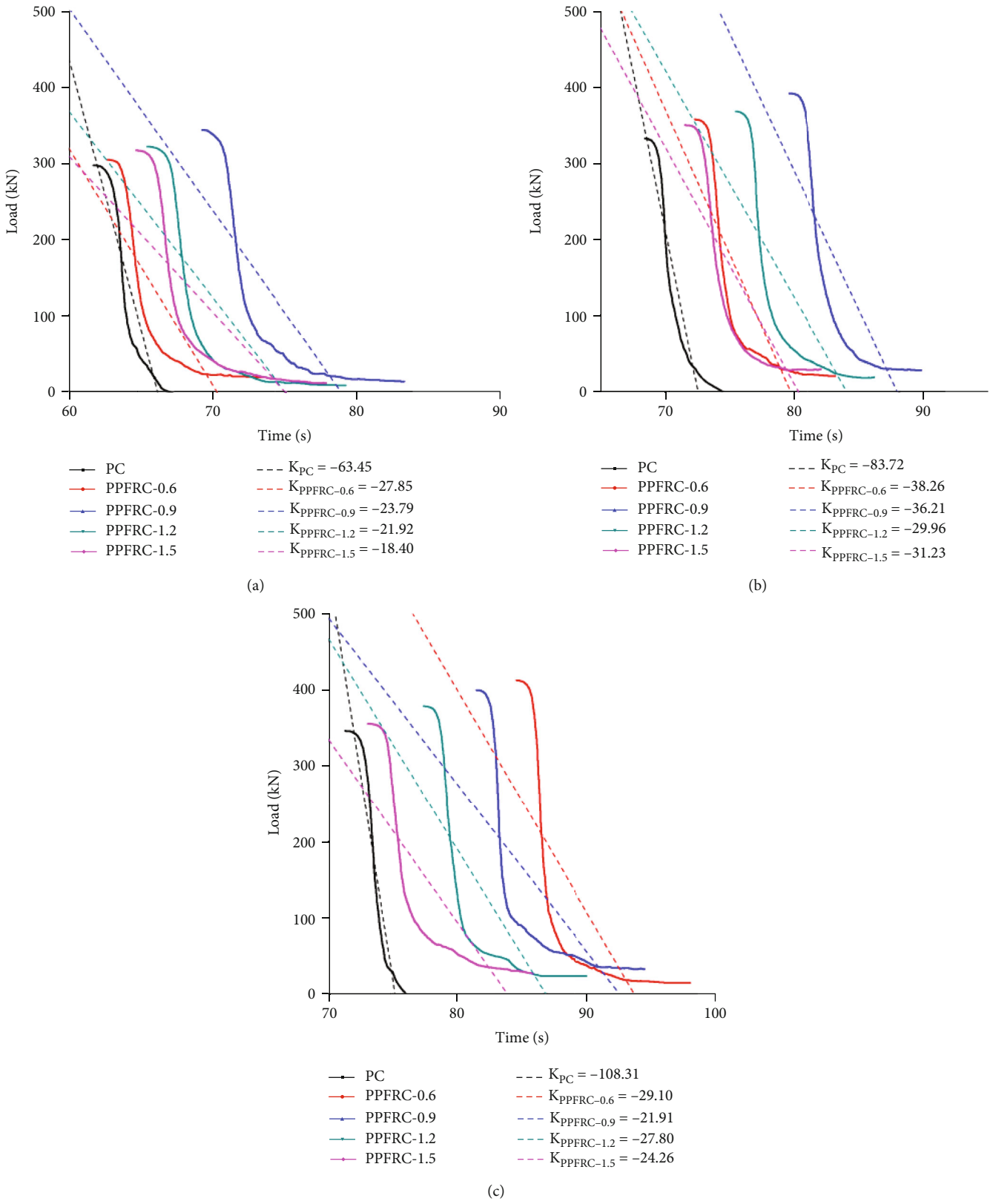

Figure 10: The descending part of compressive load–time curves: (a) 14 days, (b) 28 days, and (c) 60 days.

it is clear that the fiber is located in the crack and creates the connection bridges in Figure 7, and fibers prevent the separation of concrete pieces after cracking. The SEM images of PC and PPFRC are illustrated in Figure 8. The observation of the fragment surface by SEM captured at the same magnifications can observe that the cement paste around the fibers

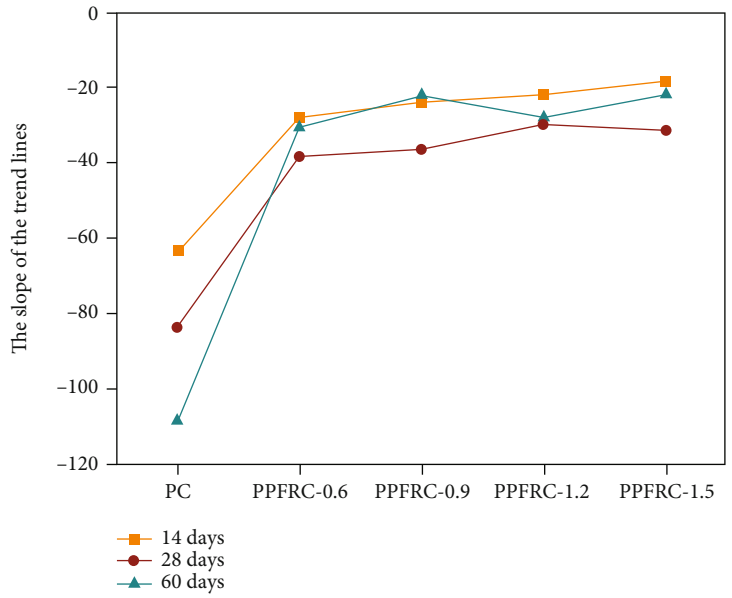

Figure 11: Slopes of the trend line of descent stage of load–time curves at 14, 28, and 60 days of curing.

Table 5: The compressive strength of PC and PPFRC at 14, 28, and 60 days of curing.

Type	Compressive strength (MPa)							
	14 days	% of increase	28 days	% of increase	60 days	% of increase	% of increase from 14 to 28 days	% of increase from 28 to 60 days
PC	29.79	—	33.29	—	34.70	—	11.75	4.24
PPFRC-0.6	30.49	2.35	35.79	7.51	41.31	19.05	17.38	15.42
PPFRC-0.9	34.43	15.58	39.20	17.75	40.01	15.30	13.85	2.07
PPFRC-1.2	32.25	8.26	36.83	10.63	37.90	9.22	14.20	2.91
PPFRC-1.5	31.76	6.61	35.03	5.23	35.63	2.68	10.30	1.71

was more compact. Random superposition strengthening effect with a large number of PPF distributed in the concrete matrix and aggregate interface may be an important source of PPF to improve the microstructure of concrete.

3.1.3. Compressive Properties. Figure 9 shows the load–time curves of PPFRC with different fiber content and PC at different curing ages. The curves were the average of nine identical mixture specimens, and the average compressive load–time curves of PC and PPFRC at 14, 28, and 60 days of curing are presented in Figure 9. Figure 10 shows the curve after the peak load in the load–time curves and the trend lines of the curves.

The peak load of the resulting PPFRC mixtures is always higher than PC. F_{fc}, the load that the first crack occurred, is about 80% of the peak load. The PPF addition may limit crack propagation by bridging cracks. These fibers provide obvious resistance to stress after the cracks appear. This ability may be the reason for the increase in the F_{fc} value of PPFRC. It can be seen from Figure 9 that PC fails in a brittle manner once the occurrence of the ultimate load, which implies the high brittleness nature of PC. The PPFRC does not have a sudden decrease but gradually decreases and tends to stabilize in intensity after reaching the peak load, showing a certain destruction process. This phenomenon indicates that the PPFRC can still bear certain loads after failure, increasing the ductility of concrete under compressive failure. After adding PPF, it was obvious that the addition of PPF mainly affected the descending part of compressive load–time curves. However, regardless of the fiber content, descending portion of those curves is not much different. Figure 8 also shows that an increase in PPF content increased the total area under those curves. This indicated that adding PPF in PC could decrease its brittleness texture and increase its ductility under compressive loading.

Figure 11 is the slope curves of the trend lines in Figure 9. Regardless of the PPF contents, the PPFRC slope is not much different and far below PC. After the maximum load, fibers share part of the energy, restraining the formation and

Table 6: The CFEC, CCEC, ECEC, CEC, FCEC, and CTI values of PC and PPFRC at 14, 28, and 60 days of curing.

Parameters	Group				
	PC	PPFRC-0.6	PPFRC-0.9	PPFRC-1.2	PPFRC-1.5
14 days					
F_{fc} (kN)	253.3	260.88	285.60	270.17	267.82
F_{Max} (kN)	297.9	304.93	344.33	322.53	317.57
CFEC (kN·s)	6534.64	6771.21	8092.59	7253.51	7116.87
CCEC (kN·s)	2775.97	2892.76	3998.34	3429.96	3285.14
ECEC (kN·s)	9310.61	9663.97	12080.93	10683.47	10402.01
CEC (kN·s)	10065.01	10657.21	13425.79	11852.86	11554.81
FCEC (kN·s)	754.79	993.24	1344.86	1169.39	1152.80
CTI (-)	1.54	1.57	1.66	1.63	1.62
28 days					
F_{fc} (kN)	275.60	292.50	315.91	298.04	289.53
F_{Max} (kN)	332.85	357.92	391.96	368.25	350.34
CFEC (kN·s)	7459.30	8490.33	9900.24	8781.66	8283.73
CCEC (kN·s)	3891.77	4628.63	5898.43	5077.61	4279.97
ECEC (kN·s)	11351.07	13118.96	15798.67	13859.27	12563.45
CEC (kN·s)	12057.93	14168.84	17008.35	14912.78	13709.21
FCEC (kN·s)	706.86	1049.44	1209.68	1053.54	1145.76
CTI (-)	1.62	1.67	1.72	1.70	1.65
60 days					
F_{fc} (kN)	290.11	330.00	323.59	310.16	298.15
F_{Max} (kN)	347.02	413.14	400.11	379.04	356.28
CFEC (kN·s)	8419.61	10863.61	10401.19	9593.42	8869.85
CCEC (kN·s)	4004.58	6747.31	59530.88	5187.46	4233.33
ECEC (kN·s)	12424.19	17610.92	16355.07	14780.88	13103.18
CEC (kN·s)	13234.84	18755.04	17666.69	15988.49	14468.74
FCEC (kN·s)	810.65	1144.09	1311.62	1207.61	1365.53
CTI (-)	1.57	1.73	1.70	1.67	1.63

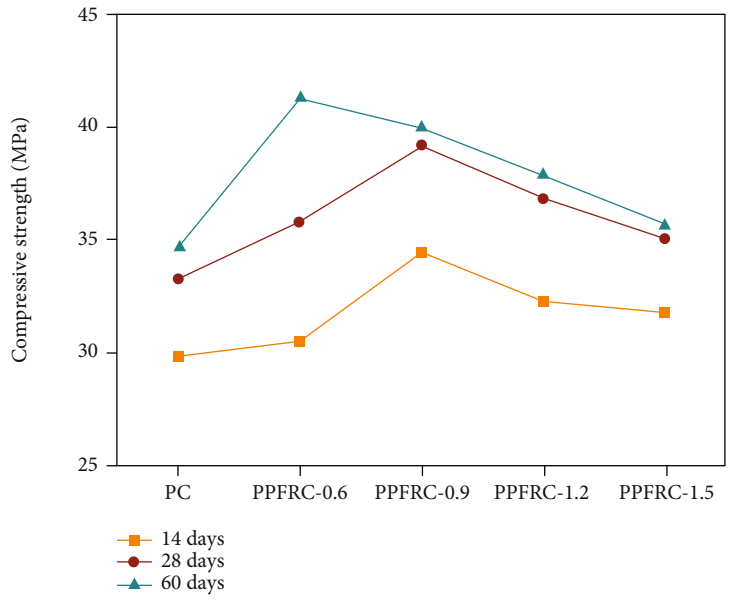

Figure 12: Compressive strength at 14, 28, and 60 days of curing.

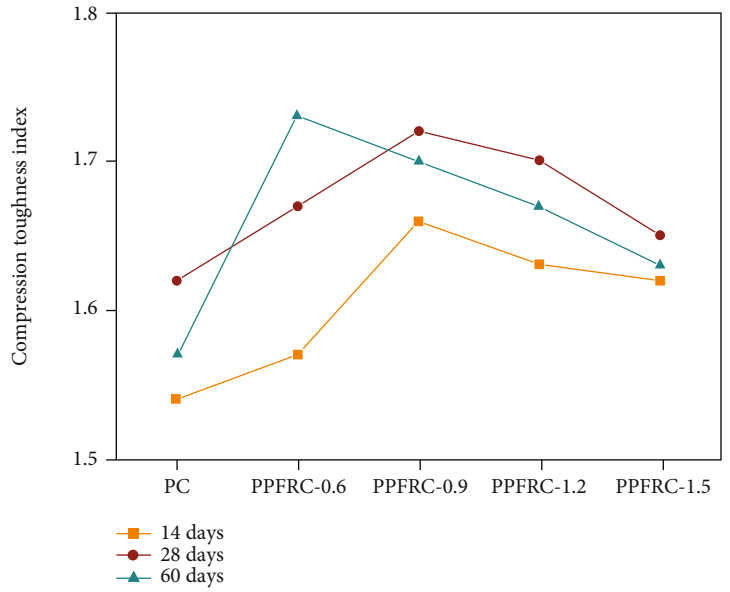

Figure 13: Compressive toughness index at 14, 28, and 60 days of curing.

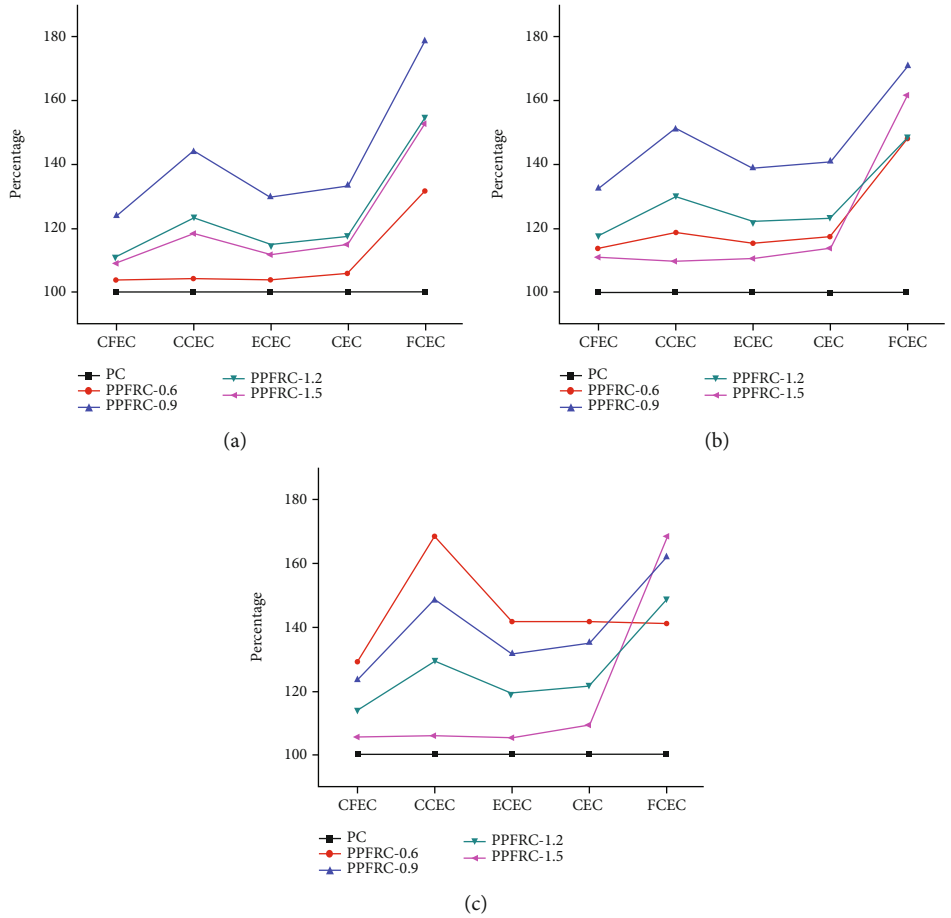

Figure 14: Comparison of PC and PPFRC energy absorption: (a) 14 days, (b) 28 days, and (c) 60 days.

development of cracks during concrete compressive. In other words, PPFRC has the ability to suppress the final failure of concrete and can prolong the damage time.

The compressive strength (CS) is calculated from the maximum load from the compressive load–time curves, and the CS of PC and PPFRC are shown in Table 5. The following parameters are defined according to the load–time curve obtained from the compressive test: (1) The area under the load–time curve from the origin to the appearance of the first crack is defined as the compressive first crack energy absorption capacity (CFEC). (2) The area under the curve from the first crack to the peak load is the compressive cracked energy absorption capacity (CCEC). (3) The area under the curve from the origin to the peak load is defined as the effective compressive energy absorption capacity (ECEC). (4) The total area under the entire curve is the compressive energy absorption capacity (CEC). (5) The area under the curve after the peak load is the failure compressive energy absorption capacity (FCEC). (6) CEC/CFEC is defined as the compressive toughness index (CTI) [7, 9, 12]. According to the definition of the above parameters, the values of the CFEC, CCEC, ECEC, CEC, FCEC, and CTI for PPFRC-0.6, PPFRC-0.9, PPFRC-1.2, and PPFRC-1.5 are calculated, and the results are listed in Table 6.

The compressive strength of PPFRC illustrates the distinct effect PPF on the composites. The strength was measured after 14, 28, and 60 days of curing. Compared to PC (see Figure 12), the CS of PPFRC is always higher than PC. The reason that increased the CS of concrete may be that fibers will disperse into a three-dimensional fiber network in the concrete, limiting the transverse deformation of concrete. The strength of PPFRC-0.6 is the most obvious improvement. The 28-day strength of PPFRC-0.6 enhanced approximately by 17.38% compared to 14-day strength and 60-day strength enhanced approximately by 15.42% compared to 28-day strength. The CS of PPFRC-0.9 is maximal at 14 and 28 days; however, after 60 days, CS of PPFRC-0.6 is ultimate. The 14-day strength of PPFRC-0.9 is increased by 15.58% than that of PC, and the 28-day strength of PPFRC-0.9 is increased by 17.75% than PC. The 60-day strength of PPFRC-0.6 is increased by 19.05% than PC.

Figure 13 shows the influence of PPF content on compressive toughness index. As can be seen, the toughness index of PPFRC is significantly higher than PC. The toughness index increases first and then decreases with the increase of PPF content, and the maximum value is PPFRC-0.9 at 14 and 28 days of curing; however, the maximum value is PPFRC-0.6 at 60 days. The 28-day CTI of PPFRC-1.2 and PPFRC-1.5 is slightly lower than that of PPFRC-0.9. The values of PPFRC-0.6 are slightly lower than that of PPFRC-1.5. PPF acts as a bridge across transverse cracks, relieves stress concentration at the crack tip, and increases the expansion resistance of cracks. This ability may be the cause of increased CTI of PPFRC.

Assuming the PC is 100, the comparisons of CFEC, CCEC, ECEC, CEC, and FCEC of PC, PPFRC-0.6, PPFRC-0.9, PPFRC-1.2, and PPFRC-1.5 are shown in Figure 13. In addition, compared with PC, the CFEC, CCEC, ECEC, CEC, and FCEC of PPFRC are all higher (Figure 13), wherein the values of PPFRC-0.9 are maximal at 14 and 28 days. The values of PPFRC-1.2 are close to PPFRC-1.5, and the other values of PPFRC-0.6 are almost similar to PC except for the FCEC at 14 days of curing. The FCEC value of PPFRC is larger than PC. The 28-day FCEC value of PPFRC-1.5 exceeds PPFRC-0.6 and PPFRC-1.2, and the FCEC value of PPFRC-1.5 is supreme after 60 days; however, the FCEC value of PPFRC-0.6 is lower than PPFRC-0.9, PPFRC-1.2, and PPFRC-0.5.

Figure 15: Uniaxial compression test.

In Figure 14(a), PPFRC-0.9 showed the highest values, which was followed by PPFRC-1.2, PPFRC-1.5, and PPFRC-0.6, wherein the values of PPFRC-1.2 is slightly higher than PPFRC-1.5. In Figure 14(b) the CFEC, CCEC, ECEC, and CEC values of PPFRC-0.6 exceeded PPFRC-1.5, and in Figure 14(c), the CFEC, CCEC, ECEC, and CEC values of PPFRC-0.6 exceeded PPFRC-0.6 which become the maximum. The FCEC values have different changes at 14, 28, and 60 days. The reason is that there is a difference in the length of the tail in the falling section of the load–time curves.

3.2. Uniaxial Compression Test

3.2.1. Test Phenomena and Failure Patterns. The specimens used in the uniaxial compression test are prismatic, showing more obvious brittleness than those in the cube compression test. The uniaxial compression test is shown in Figure 15. During the loading process of the test, PC specimens appeared spalling phenomenon with large and

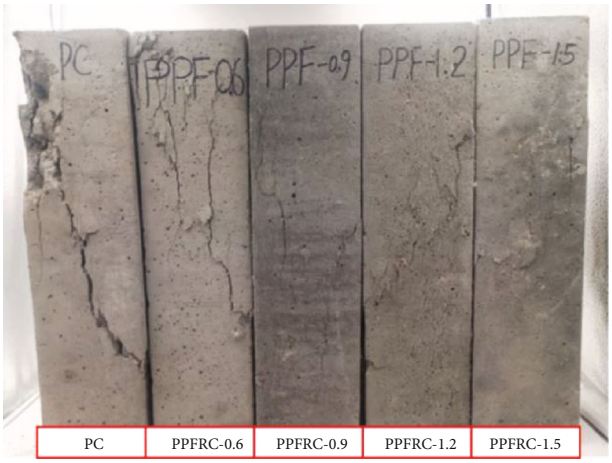

Figure 16: Uniaxial compression failure morphology of specimens at 28 days of curing age (sample 1).

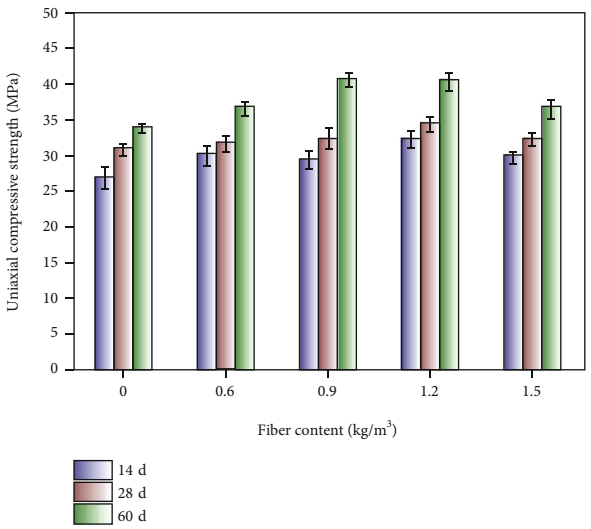

Figure 17: Uniaxial compression strength of PC and PPFRC at different curing ages.

Table 7: Growth rate of uniaxial compression strength of PC and PPFRC at different curing ages.

Type	Uniaxial compression strength (MPa)							
	14 days	% of increase	28 days	% of increase	60 days	% of increase	% of increase from 14 to 28 days	% of increase from 28 to 60 days
PC	26.94	—	30.95	—	33.95	—	14.88	9.69
PPFRC-0.6	30.13	11.84	31.70	2.42	36.63	7.89	5.21	15.55
PPFRC-0.9	29.45	9.32	32.45	4.85	40.63	19.68	10.19	25.21
PPFRC-1.2	32.48	20.56	34.43	11.24	40.47	19.20	6.00	17.54
PPFRC-1.5	29.80	10.62	32.39	4.65	36.70	8.10	8.69	13.31

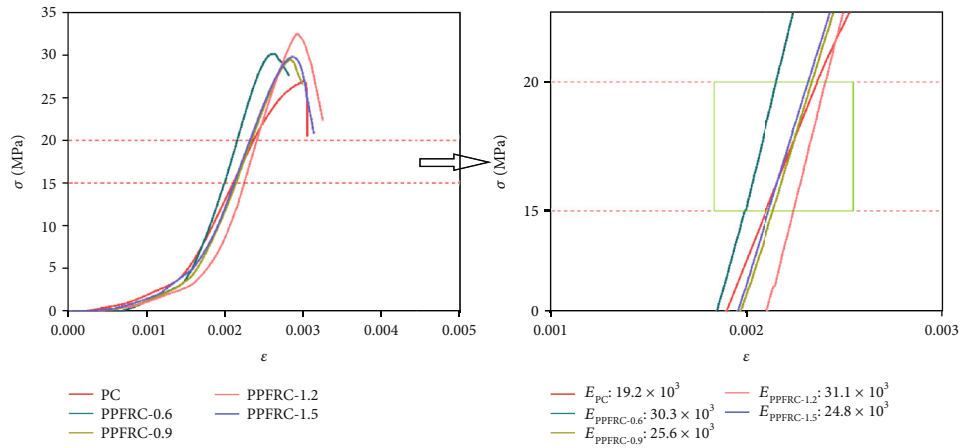

Figure 18: Uniaxial compressive stress-strain curve of PC and PPFRC at 14-day curing age.

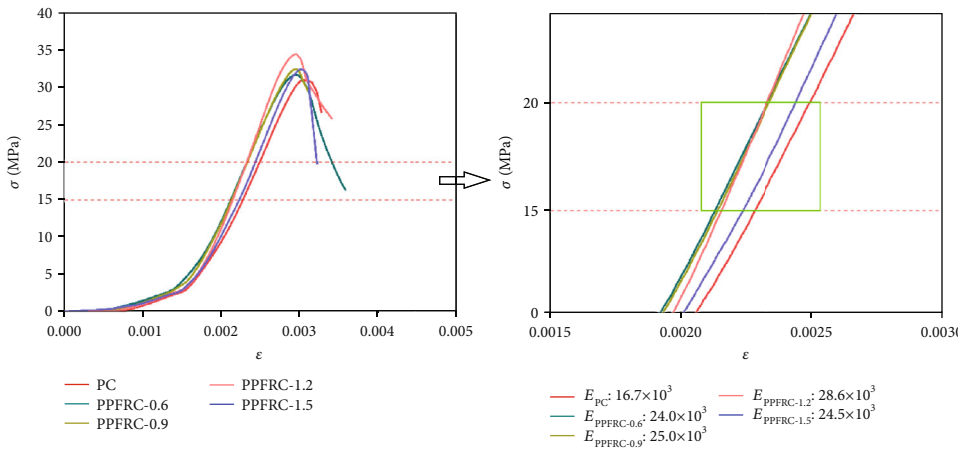

Figure 19: Uniaxial compressive stress-strain curve of PC and PPFRC at 28-day curing age.

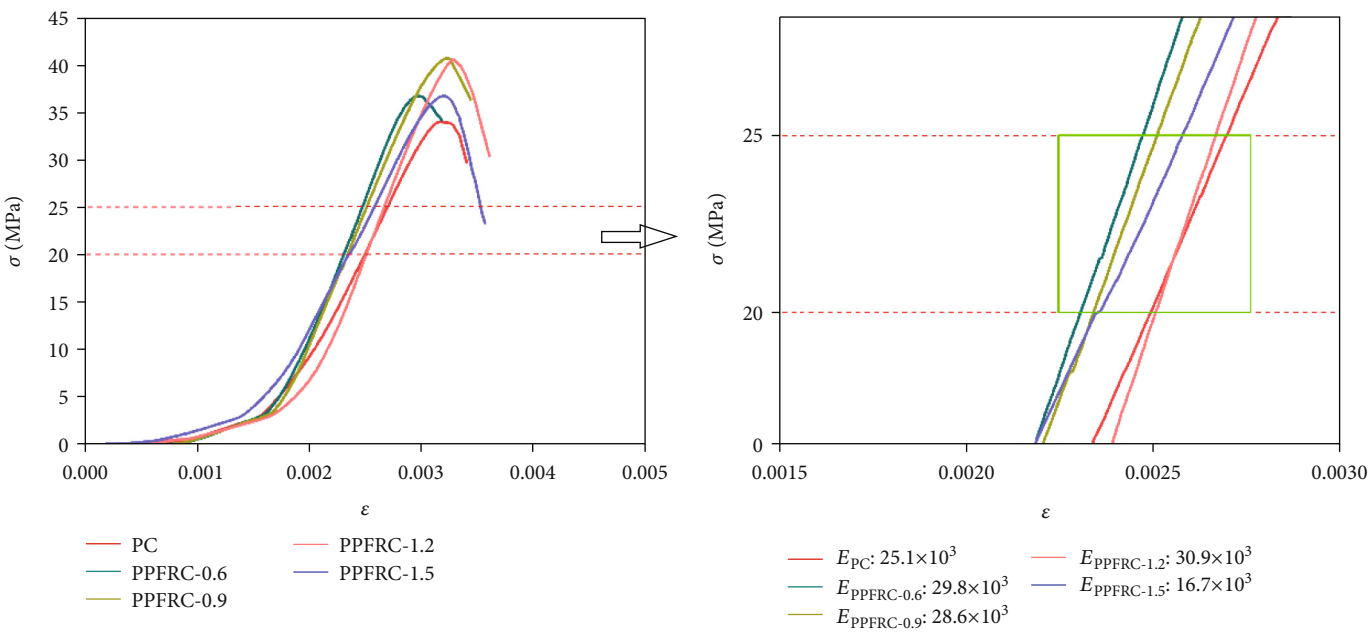

Figure 20: Uniaxial compressive stress-strain curve of PC and PPFRC at 60-day curing age.

Table 8: Parameter α_a and α_d values after improved algorithm.

Type	14 days		28 days		60 days	
	α_a	α_d	α_a	α_d	α_a	α_d
PC	2.0002910	4.0	2.0003062	3.5	2.0002882	3.0
PPFRC-0.6	2.0002687	3.5	2.0003163	3.5	2.0002378	3.0
PPFRC-0.9	2.0003526	3.5	2.0003224	3.5	2.0002456	3.0
PPFRC-1.2	2.0004011	3.5	2.0002364	3.5	2.0003046	3.0
PPFRC-1.5	2.0002566	3.5	2.0003625	3.5	2.0002695	3.0

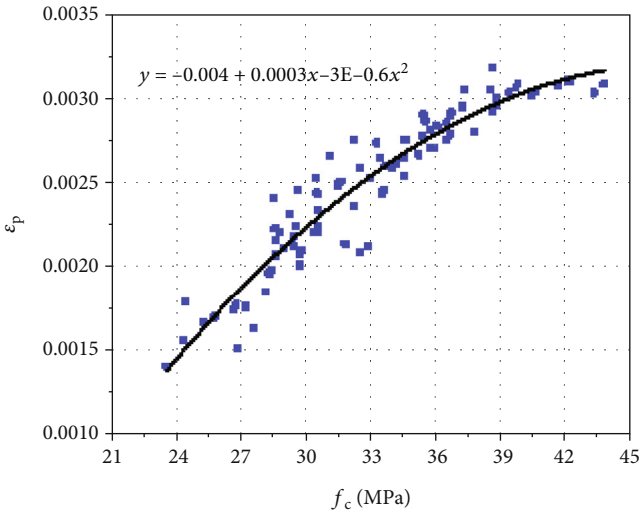

Figure 21: Relationship between peak point strain ε_p and uniaxial compressive strength f_c of PC and PPFRC.

penetrating cracks and shear failure. The specimens were separated into two parts and the damage was sudden. The PPFRC specimens showed no obvious spalling phenomenon, but some small cracks, with good integrity and ductility. This is because the bridging effect of PPF limits the generation and development of cracks. As can be seen from Figure 16, PPF can play a good role in cracking resistance of concrete in the process of uniaxial compression failure. With the increase of fiber content, the integrity of the specimen becomes better. This is closely related to the bridging function of fiber between matrices.

3.2.2. Analysis of Experimental Results. Figure 17 shows the change trend of uniaxial compressive strength at different curing ages of PPFRC specimens with different dosage. It can be seen from the figure that the uniaxial compressive strength of concrete increases after fiber is added, and the uniaxial compressive strength of PPFRC specimens increases first and then decreases with the increase of fiber dosage. As the age increases, PPF has a significant strengthening effect on the late strength of concrete, improving the continuity and integrity of concrete. Uniaxial compression strength and growth rate of specimens with different curing ages and different dosage of PPFRC are summarized in Table 7. Then, curing age is 14 days and the dosage is 1.2 kg/m^3, and the PPFRC uniaxial compression strength is the largest, 20.56% higher than PC. When the dosage is 0.9 kg/m^3, the PPFRC uniaxial compression strength increases the least, 9.32% higher than PC. Then, curing age is 28 days and the dosage is 1.2 kg/m^3, and the PPFRC uniaxial compressive strength is the largest, 11.24% higher than PC. When the dosage is 0.9 kg/m^3, the PPFRC uniaxial compressive strength is the second, 4.85% higher than PC. The uniaxial compression strength of PPFRC was the highest when the age was 60 days and the dosage was 0.9 kg/m^3, 19.68% higher than PC. A comprehensive comparison of the uniaxial compressive strength of the three ages shows that the fiber content of 1.2 kg/m^3 has the best effect on the uniaxial compressive strength of concrete, and the uniaxial compressive strength of the two ages increases the most significantly.

3.2.3. Stress-Strain Constitutive Model of Uniaxial Compression. Figures 18–20 show the uniaxial stress-strain curves of PC, PPFRC-0.6, PPFRC-0.9, PPFRC-1.2, and PPFRC-1.5 at curing ages of 14 days, 28 days, and 60 days. It can be seen that the stress-strain curve of PPFRC specimen is similar to that of PC. It indicates that the failure mode of PPFRC prism specimen is the same as that of PC. The specimens failed quickly after reaching the ultimate load, so only a part of the descending section of the curve.

The steady rising stage of the curve is a straight section, whose slope is approximately equal to the elastic modulus value. The slope of the linear section of the uniaxial compressive stress-strain curve is calculated (at 14 and 28 days, the slope of the curve with a stress of 15~20 MPa is calculated; at 60 days, the slope of the curve during the stress period of 20~25 MPa is calculated). It was found that the PPFRC modulus of 1.2 kg/m^3 was the highest at 14 days, 28 days, and 60 days, with 31.1×10^3 MPa and 28.6×10^3 MPa and 30.9×10^3 MPa, respectively. At 14 days and 28 days, the elastic modulus of PC was less than PPFRC, which were 19.2×10^3 MPa and 16.7×10^3 MPa, respectively. At 60 days, only the PPFRC slope with a dosage of 1.5 kg/m^3 is less than PC.

$$\begin{cases} \sigma = \left[\alpha_a \dfrac{\varepsilon}{\varepsilon_p} + (3-2\alpha_a)\left(\dfrac{\varepsilon}{\varepsilon_p}\right)^2 + (\alpha_a - 2)\left(\dfrac{\varepsilon}{\varepsilon_p}\right)^3\right] f_c & \left(0 \le \varepsilon \le \varepsilon_p\right), \\ \sigma = \left[\dfrac{\varepsilon/\varepsilon_p}{\alpha_d\left(\varepsilon/\varepsilon_p - 1\right)^2 + \varepsilon/\varepsilon_p}\right] f_c & \left(\varepsilon_p \le \varepsilon\right). \end{cases} \tag{1}$$

In the formula, a_a is the rising section of the stress-strain curve, generally $0.5 \le \alpha_a \le 3.0$; a_d is the parameter of the falling section of the stress-strain curve, usually taking $0.4 \le \alpha_d \le 2.0$, and there is also the case of $\alpha_d = 4.0$.

Based on the uniaxial compressive stress-strain curve relationship of concrete, the values of a_a and a_d in equation (1) can be derived. The derivation process can fit the corresponding curve form according to the test data and transform the deduced problem into an optimization problem. It is assumed that the ideal value (rising segment coefficient

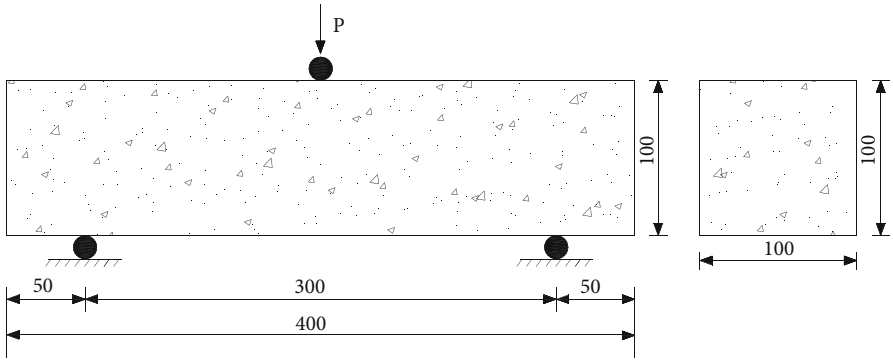

Figure 22: The schematic diagram of flexural test.

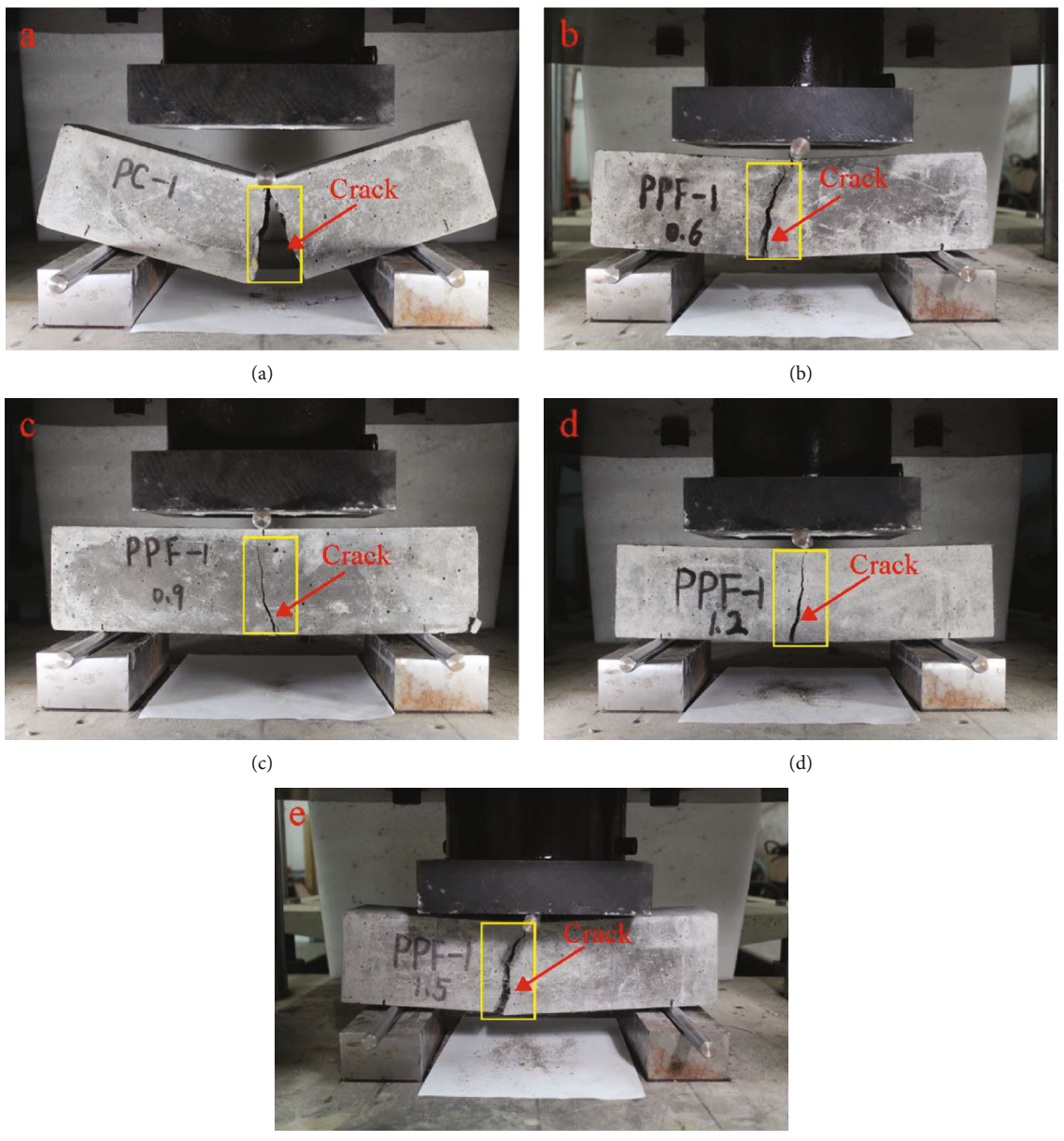

(a) (b) (c) (d) (e)

Figure 23: PC and PPFRC failure type: (a) PC (brittle) and (b~e) PPFRC (ductile).

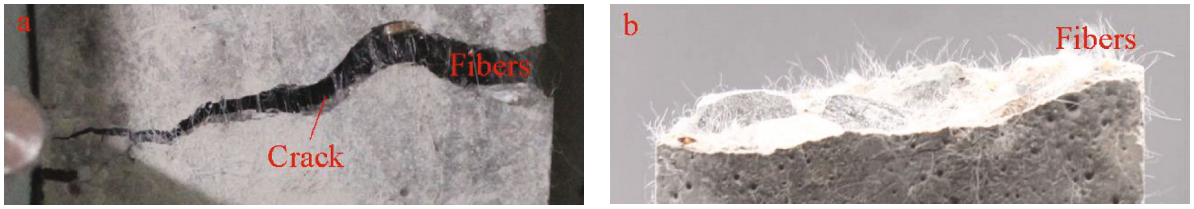

(a) (b)

Figure 24: Fibers bridging at the crack section.

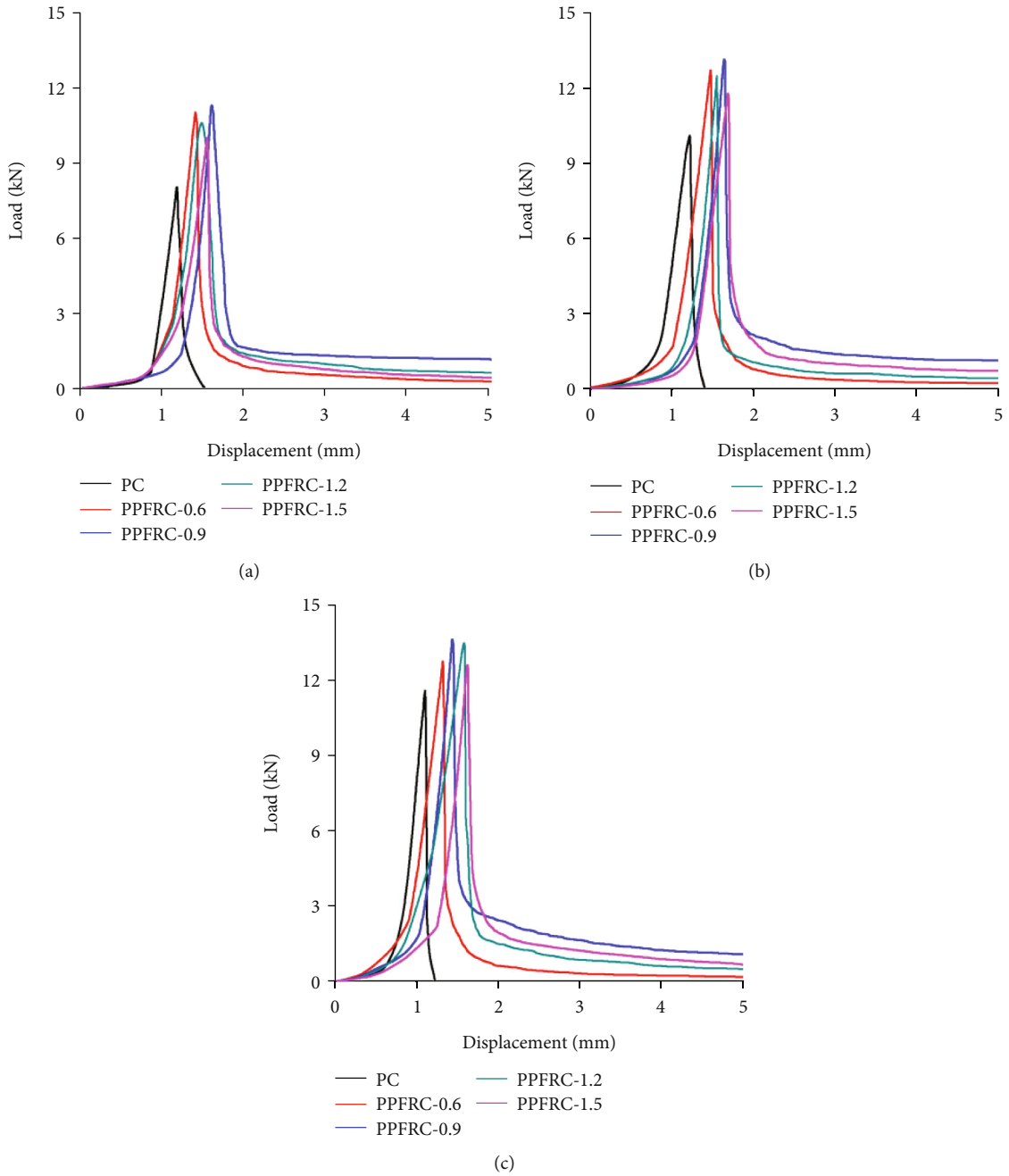

Figure 25: Load–time curves of PC and PPFRC from flexural test: (a) 14 days, (b) 28 days, and (c) 60 days.

Table 9: The flexural strength of PC and PPFRC at 14, 28, and 60 days of curing.

Type	Flexural strength (MPa)							
	14 days	% of increase	28 days	% of increase	60 days	% of increase	% of increase from 14 to 28 days	% of increase from 28 to 60 days
PC	3.63	—	4.55	—	5.20	—	25.34	14.29
PPFRC-0.6	4.95	36.36	5.72	25.71	6.13	17.88	15.56	7.17
PPFRC-0.9	5.10	40.50	5.90	29.67	6.31	21.35	15.69	6.95
PPFRC-1.2	4.88	34.44	5.65	24.18	6.08	16.92	15.78	7.61
PPFRC-1.5	4.45	22.59	5.32	16.92	5.65	8.65	19.55	6.20

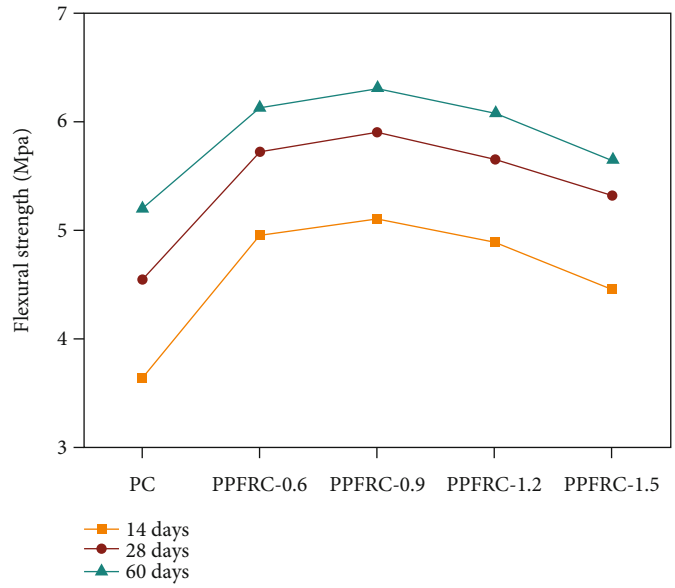

Figure 26: Flexural strength curves at 14, 28, and 60 days of curing.

a_a and descending segment coefficient a_d) satisfies the condition of the Zhenhai model. Therefore, a nonideal value must have a residual e, for the rising section curve:

$$e = \int_0^{\varepsilon_p} \left(\sigma - \left(\alpha_a \frac{\varepsilon}{\varepsilon_p} + (3 - 2\alpha_a) \left(\frac{\varepsilon}{\varepsilon_p} \right)^2 + (\alpha_a - 2) \left(\frac{\varepsilon}{\varepsilon_p} \right)^3 \right) f_c \right) d\varepsilon. \tag{2}$$

For the falling section curve,

$$e = \int_{\varepsilon_p}^{+\infty} \left(\sigma - \left(\frac{\varepsilon/\varepsilon_p}{\alpha_d (\varepsilon/\varepsilon_p - 1)^2 + \varepsilon/\varepsilon_p} \right) f_c \right) d\varepsilon. \tag{3}$$

The process of fitting the parameter values α_a and α_d is actually the process of finding the minimum value of e. Since the model of the Zhenhai model is smooth and continuous, the above problem is simplified by taking multiple sample points of the model curve, that is, for the rising section curve:

$$\min : \sum_{i=1}^{n} e_i = \sum_{i=1}^{n} \left(\sigma_i - \left(\alpha_a \frac{\varepsilon_i}{\varepsilon_p} + (3 - 2\alpha_a) \left(\frac{\varepsilon_i}{\varepsilon_p} \right)^2 + (\alpha_a - 2) \left(\frac{\varepsilon_i}{\varepsilon_p} \right)^3 \right) f_c \right). \tag{4}$$

For the falling section curve,

$$\min : \sum_{j=1}^{m} e_j = \sum_{j=1}^{m} \left(\sigma_j - \left(\frac{\varepsilon_j/\varepsilon_p}{\alpha_d (\varepsilon_j/\varepsilon_p - 1)^2 + \varepsilon_j/\varepsilon_p} \right) f_c \right). \tag{5}$$

Considering that the relationship between e and the parameter to be estimated is nonlinear, there are usually many minimum values in the search domain. The traditional optimization algorithm may not be competent. Therefore, this paper uses the improved differential evolution

algorithm proposed by Qian et al. [46]. For this optimization problem, the calculation results are shown in Table 8.

It can be seen that the regularity of the rising and falling sections of the uniaxial compressive stress-strain curve of the PPFRC specimens is basically the same, wherein α_a is approximately equal to 2 and α_d decreases with age, and its uniaxial compression stress-strain curve equation can be expressed as follows:

For rising section ($0 \le \varepsilon \le \varepsilon_p$),

$$\sigma = \left[\frac{2\varepsilon}{\varepsilon_p} - \left(\frac{\varepsilon}{\varepsilon_p}\right)^2\right] f_c. \tag{6}$$

For falling section ($\varepsilon_p \le \varepsilon$),

$$\sigma = \left[\frac{\varepsilon/\varepsilon_p}{\alpha_d\left(\varepsilon/\varepsilon_p - 1\right)^2 + \varepsilon/\varepsilon_p}\right] f_c. \tag{7}$$

In the above uniaxial compressive stress-strain constitutive model, in addition to the compressive strength f_c, the peak point strain ε_p is a key parameter. Establish the relationship between the uniaxial compressive strength f_c of the PPFRC specimen and the peak point strain ε_p, as shown in Figure 21. When the statistic data of PC and different PPPRC specimens at three curing ages were statistically found, there was a quadratic function relationship between the prism strength and the peak strain. The peak strain ε_p and the axis were obtained by fitting the experimental data. The relationship between the compressive strengths f_c is shown.

3.3. Flexural Test

3.3.1. Test Phenomena and Failure Patterns. The flexural strength of concrete is an important characteristic which significantly affects the safety and service life of concrete. The three-point bending test was carried out to evaluate the behavior of PPFRC specimens, and Figure 22 shows the schematic diagram of the three-point bending test used in this study.

Figure 23 displays the formation of the crack at the ultimate load of PC and PPFRC at 28 days, and all specimens have only one crack and located approximately in the middle. It can be observed that PPFRC specimens are held together because of the constraint effect of fibers. At the ultimate load, the crack opening widths for the specimens of PC, PPFRC-0.6, PPFRC-0.9, PPFRC-1.2, and PPFRC-1.5 were enlarged up to about 55 mm, 13 mm, 2 mm, 5 mm, and 13 mm, respectively. After flexure test, when low content PPF being in PC mixture is to bridge across the microcracks, the extra energy is consumed as the fibers were destroyed or pulled out, which leads to higher failure load and toughness of the material.

In the case of flexure test, for better observation of fibers failure, the beams of PPFRC are intentionally broken into two portions, as shown in Figure 24. It is observed that fibers with an almost uniform distribution are pulled out and fractured on the fragmented surface of specimens. By visual inspection of the fractured surfaces of the beams of PPFRC, the random distribution and dispersal of PPF were found. After the matrix cracks, the fibers can continue to bear the load. The integrity and continuity of the concrete can be improved by adding fibers. The fibers can prevent the fracture surface from being separated by bridging across the cracks when cracks appeared and propagated, bearing the load until they are pulled out of the matrix.

3.3.2. Flexural Strength. Figure 25 shows the load–displacement curves of PPFRC with different fiber contents at 14, 28, and 60 days of curing for flexure strength test. The curves were the average of nine identical specimens. As with the compression test curves, the addition of PPF affects the descending part of flexural load–displacement curves, reducing brittle of PC and increases ductility of PC. The flexure strengths and percentage increase of PPFRC with different fiber contents at 14, 28, and 60 days of curing are summarized in Table 9. In Figure 24, the displacements corresponding to the peak load of the specimens containing PPF were greater, showing a higher peak load and long postpeak curve. The flexural strength curves are shown in Figure 26, and the increasing trend of the flexural strengths of PC and PPFRC at the three ages is approximately the same. It can be seen that the mechanical properties of concrete will not improve with the increase of PPF content. A small amount of PPF can play an effective bridging role in the slurry. However, when the content of PPF is too large, the fiber is not easy to disperse, and it is easy to knot in the slurry to form cavities or cracks. This will weaken the strength of concrete per unit area to a certain extent [47]. The flexural strength of concrete is calculated according to the following equation:

$$f = \frac{3PL}{2bh^2}, \tag{8}$$

where P is the maximum load (kN), L is the span of the beam, L is 3 h, b is the beam width, and h is the beam depth.

4. Conclusions

In this study, compressive and flexural tests were conducted on PC, PPFRC-0.6, PPFRC-0.9, PPFRC-1.2, and PPFRC-1.5 at different curing ages. At the same mix ratio, with the increase of fiber content, especially over 1.2 kg/m^3, the fluidity of the mixture is very low, resulting in the mixture being difficult to deal with. The following conclusions were obtained through compressive and flexural tests.

(1) The compressive test shows that the compressive strengths of PPFRC with different fiber contents are all higher than that of PC, and the compressive strength of PPFRC-0.9 is the highest at 14 and 28 days. After 28 days of curing, compared with PC, the strength of PPFRC-0.6, PPFRC-0.9, PPFRC-1.2, and PPFRC-1.5 increased by 7.51%, 17.75%, 10.63%, and 5.23%, respectively. However, after 60 days of curing, the compressive strength of PPFRC-0.6 exceeds PPFRC-0.9 to become the highest

(2) Load–time curve was obtained from the compressive test. The first crack energy absorption capacity and

toughness index were calculated. It is found that the CFEC and CTI of PPFRC are both higher than PC. When the PPF content is 0.9 kg/m^3, the CFEC and CTI are the largest at 14- and 28-day ages. If a crack exists in the specimen, a bridging effect is observed in the PPFRC and the PPF absorbs the compressive crack energy. The enhancement of the toughness behavior is owed to the crack bridging effect of fibers in impeding the development of cracks

(3) The flexural test results indicated that the addition of PPF could significantly increase the flexural strength. For instance, when adding 0.9 kg/m^3 fibers to PC, the PPFRC specimens show the highest flexural strength with the value of 5.10 MPa, 5.90 MPa, and 6.31 MPa at 14 days, 28 days, and 60 days, which are 40.50%, 29.67%, and 21.35% higher than PC, respectively

(4) The test results show that low-content PPF can effectively improve the compressive strength, the compressive first crack energy absorption capacity, the compressive toughness index of concrete mixture, and flexural strength. This is of great significance to the application of PPF in concrete. The use of low content (0.6~0.9 kg/m^3) PPF can not only avoid harmful pores and cracks in the concrete but also obtain better workability and improve the performance of the concrete

Abbreviations

PC: Plain concrete
PPF: Polypropylene fiber
PPFRC: PPF-reinforced concrete
SEM: Scanning electron microscope
CS: Compressive strength
CFEC: Compressive first crack energy absorption capacity
CCEC: Compressive cracked energy absorption capacity
ECEC: Effective compressive energy absorption capacity
CEC: Compressive energy absorption capacity
FCEC: Failure compressive energy absorption capacity
CTI: Compressive toughness index.

Data Availability

The experimental data used to support the findings of this study are included within the article.

Conflicts of Interest

The authors declare no conflict of interest.

Acknowledgments

This study was financially supported by the National Natural Science Foundation of China (Nos. 51722907, 51679197, and 51579207).

References

[1] P. Zhang, K. Wang, J. Wang, J. Guo, and Y. Ling, "Mechanical properties and prediction of fracture parameters of geopolymer/alkali-activated mortar modified with PVA fiber and nano-SiO_2," *Ceramics International*, vol. 46, no. 12, pp. 20027–20037, 2020.

[2] I. Khan, A. Castel, and R. I. Gilbert, "Tensile creep and early-age concrete cracking due to restrained shrinkage," *Construction and Building Materials*, vol. 149, pp. 705–715, 2017.

[3] D. H. Nguyen, V. Dao, and P. Lura, "Tensile properties of concrete at very early ages," *Construction & Building Materials*, vol. 134, no. MAR.1, pp. 563–573, 2017.

[4] R. Abousnina, H. I. Alsalmi, A. Manalo et al., "Effect of short fibres in the mechanical properties of geopolymer mortar containing oil-contaminated sand," *Polymers*, vol. 13, no. 17, article 3008, 2021.

[5] P. Yu, A. Manalo, W. Ferdous, R. Abousnina, and P. Schubel, "Investigation on the physical, mechanical and microstructural properties of epoxy polymer matrix with crumb rubber and short fibres for composite railway sleepers," *Construction and Building Materials*, vol. 295, no. 2, article 123700, 2021.

[6] C. Saketh, J. M. Patel, M. Rajesh, G. Sadanand, and M. Manoj, "Statistical analysis of polypropylene fibre reinforced concrete," *International Journal of Advance Research, Ideas and Innovations in Technology*, vol. 3, no. 3, pp. 518–532, 2017.

[7] A. Zia and M. Ali, "Behavior of fiber reinforced concrete for controlling the rate of cracking in canal-lining," *Construction and Building Materials*, vol. 155, no. nov.30, pp. 726–739, 2017.

[8] Z. Ranachowski and K. Schabowicz, "The contribution of fiber reinforcement system to the overall toughness of cellulose fiber concrete panels," *Construction and Building Materials*, vol. 156, pp. 1028–1034, 2017.

[9] M. Khan and M. Ali, "Effectiveness of hair and wave polypropylene fibers for concrete roads," *Construction & Building Materials*, vol. 166, pp. 581–591, 2018.

[10] Z. Gao, P. Zhang, J. Wang, K. Wang, and T. Zhang, "Interfacial properties of geopolymer mortar and concrete substrate: effect of polyvinyl alcohol fiber and nano-SiO_2 contents," *Construction and Building Materials*, vol. 315, article 125735, 2022.

[11] P. Zhang, Z. Gao, J. Wang, and K. Wang, "Numerical modeling of rebar-matrix bond behaviors of nano-SiO_2 and PVA fiber reinforced geopolymer composites," *Ceramics International*, vol. 47, no. 8, pp. 11727–11737, 2021.

[12] M. Khan and M. Ali, "Use of glass and nylon fibers in concrete for controlling early age micro cracking in bridge decks," *Construction & Building Materials*, vol. 125, pp. 800–808, 2016.

[13] P. Zhang, Q. Li, and H. Zhang, "Combined effect of polypropylene fiber and silica fume on mechanical properties of concrete composite containing fly ash," *Journal of Reinforced Plastics & Composites*, vol. 30, no. 16, pp. 1349–1358, 2011.

[14] N. Flores Medina, G. Barluenga, and F. Hernandez-Olivares, "Combined effect of polypropylene fibers and silica fume to improve the durability of concrete with natural pozzolans blended cement," *Construction & Building Materials*, vol. 96, pp. 556–566, 2015.

[15] B. Gonzalo, "Fiber-matrix interaction at early ages of concrete with short fibers," *Cement and Concrete Research*, vol. 40, no. 5, pp. 802–809, 2010.

[16] N. Banthia and R. Gupta, "Influence of polypropylene fiber geometry on plastic shrinkage cracking in concrete," *Cement & Concrete Research*, vol. 36, no. 7, pp. 1263–1267, 2006.

[17] D. Saje, B. Bandelj, J. Sustersic, J. Lopatic, and F. Saje, "Shrinkage of polypropylene fiber-reinforced high-performance concrete," *Journal of Materials in Civil Engineering*, vol. 23, no. 7, pp. 941–952, 2011.

[18] K. Behfarnia and A. Behravan, "Application of high performance polypropylene fibers in concrete lining of water tunnels," *Materials & Design*, vol. 55, no. mar., pp. 274–279, 2014.

[19] M. Briffaut, F. Benboudjema, and L. D'Aloia, "Effect of fibres on early age cracking of concrete tunnel lining. Part I: laboratory ring test," *Tunnelling and Underground Space Technology*, vol. 59, pp. 215–220, 2016.

[20] A. Nobili, L. Lanzoni, and A. M. Tarantino, "Experimental investigation and monitoring of a polypropylene-based fiber reinforced concrete road pavement," *Construction and Building Materials*, vol. 47, no. 10, pp. 888–895, 2013.

[21] M. Pourbaba, E. Asefi, H. Sadaghian, and A. Mirmiran, "Effect of age on the compressive strength of ultra-high-performance fiber-reinforced concrete," *Construction and Building Materials*, vol. 175, pp. 402–410, 2018.

[22] M. R. Garcez, A. B. Rohden, and L. Godoy, "The role of concrete compressive strength on the service life and life cycle of a RC structure: case study," *Journal of Cleaner Production*, vol. 172, pp. 27–38, 2018.

[23] M. Li, H. Hao, Y. Shi, and Y. Hao, "Specimen shape and size effects on the concrete compressive strength under static and dynamic tests," *Construction and Building Materials*, vol. 161, no. FEB.10, pp. 84–93, 2018.

[24] P. Jamsawang, P. Voottipruex, and S. Horpibulsuk, "Flexural strength characteristics of compacted cement-polypropylene fiber sand," *Journal of Materials in Civil Engineering*, vol. 27, no. 9, 2015.

[25] Z. Sun and Q. Xu, "Microscopic, physical and mechanical analysis of polypropylene fiber reinforced concrete," *Materials Science & Engineering A*, vol. 527, no. 1-2, pp. 198–204, 2009.

[26] E. Mohseni, M. M. Khotbehsara, F. Naseri, M. Monazami, and P. Sarker, "Polypropylene fiber reinforced cement mortars containing rice husk ash and nano-alumina," *Construction & Building Materials*, vol. 111, pp. 429–439, 2016.

[27] Y. Xue, J. Liu, X. Liang, S. Wang, and Z. Ma, "Ecological risk assessment of soil and water loss by thermal enhanced methane recovery: numerical study using two-phase flow simulation," *Journal of Cleaner Production*, vol. 334, article 130183, 2022.

[28] A. A. Ramezanianpour, M. Esmaeili, S. A. Ghahari, and M. H. Najafi, "Laboratory study on the effect of polypropylene fiber on durability, and physical and mechanical characteristic of concrete for application in sleepers," *Construction & Building Materials*, vol. 44, no. jul., pp. 411–418, 2013.

[29] L. I. Bei-Xing, M. X. Chen, F. Cheng, and L. P. Liu, "The mechanical properties of polypropylene fiber reinforced concrete," *Journal of Wuhan University Technology*, vol. 19, no. 3, pp. 68–71, 2004.

[30] Y. Choi and R. L. Yuan, "Experimental relationship between splitting tensile strength and compressive strength of GFRC and PFRC," *Cement & Concrete Research*, vol. 35, no. 8, pp. 1587–1591, 2005.

[31] J. P. Won, C. G. Park, S. W. Lee, C. I. Jang, and C. Won, "Effect of crimped synthetic fibre surface treatments on plastic shrinkage cracking of cement-based composites," *Magazine of Concrete Research*, vol. 60, no. 6, pp. 421–427, 2008.

[32] T. Simões, H. Costa, D. Dias-da-Costa, and E. Júlio, "Influence of fibres on the mechanical behaviour of fibre reinforced concrete matrixes," *Construction & Building Materials*, vol. 137, no. Complete, pp. 548–556, 2017.

[33] S. Zhang and B. Zhao, "Influence of polypropylene fibre on the mechanical performance and durability of concrete materials," *European Journal of Environmental and Civil Engineering*, vol. 16, no. 10, pp. 1269–1277, 2012.

[34] K. Behfarnia and M. Rostami, "Mechanical properties and durability of fiber reinforced alkali activated slag concrete," *Journal of Materials in Civil Engineering*, vol. 29, no. 12, pp. 04017231.1–04017231.9, 2017.

[35] M. Nili, A. Azarioon, A. Danesh, and A. Deihimi, "Experimental study and modeling of fiber volume effects on frost resistance of fiber reinforced concrete," *International Journal of Civil Engineering*, vol. 16, no. 3, pp. 263–272, 2018.

[36] P. Hou, Y. Xue, F. Gao et al., "Effect of liquid nitrogen cooling on mechanical characteristics and fracture morphology of layer coal under Brazilian splitting test," *International Journal of Rock Mechanics and Mining Sciences*, vol. 151, article 105026, 2022.

[37] Q. Fu, D. Niu, J. Zhang, D. Huang, and M. Hong, Eds., "Impact response of concrete reinforced with hybrid basalt-polypropylene fibers," *Powder Technology An International Journal on the Science & Technology of Wet & Dry Particulate Systems*, vol. 326, pp. 411–424, 2018.

[38] A. M. Lopez-Buendia, M. Romero-Sánchez, V. Climent, and C. Guillem, "Surface treated polypropylene (PP) fibres for reinforced concrete," *Cement & Concrete Research*, vol. 54, pp. 29–35, 2013.

[39] F. L. Gayarre, L. C. Perez, M. A. S. Lopez, and A. D. Cabo, "The effect of curing conditions on the compressive strength of recycled aggregate concrete," *Construction & Building Materials*, vol. 53, pp. 260–266, 2014.

[40] A. M. Zeyad, "Effect of curing methods in hot weather on the properties of high-strength concretes," *Journal of King Saud University*, vol. 31, no. 3, pp. 218–223, 2019.

[41] R. Nehvi, P. Kumar, and U. Z. Nahvi, "Effect of different percentages of polypropylene fibre (Recron 3s) on the compressive, tensile and flexural strength of concrete," *International Journal of Engineering & Technical Research*, vol. V5, no. 11, 2016.

[42] X. Shao, "experiments for strength properties of polypropylene fiber-reinforced concrete," *Advanced Materials Research*, vol. 194-196, pp. 1030–1034, 2011.

[43] A. N. Ede and A. O. Ige, "Optimal polypropylene fiber content for improved compressive and flexural strength of concrete," *IOSR Journal of Mechanical and Civil Engineering*, vol. 11, no. 3, pp. 129–135, 2014.

[44] Z. Guo, "Various structural concrete," in *Principles of Reinforced Concrete*, Elsevier B.V., 2014.

[45] L. Guoming, C. Weimin, and C. Lianjun, "Investigating and optimizing the mix proportion of pumping wet-mix shotcrete with polypropylene fiber," *Construction & Building Materials*, vol. 150, pp. 14–23, 2017.

[46] W. Qian, J. Chai, Z. Xu, and Z. Zhang, "Differential evolution algorithm with multiple mutation strategies based on roulette wheel selection," *Applied Intelligence: The International Journal of Artificial Intelligence, Neural Networks, and Complex Problem-Solving Technologies*, vol. 48, no. 10, pp. 3612–3629, 2018.

[47] A. S. M. Akid, S. Hossain, M. I. U. Munshi et al., "Assessing the influence of fly ash and polypropylene fiber on fresh, mechanical and durability properties of concrete," *Journal of King Saud University - Engineering Sciences*, vol. 33, 2021.